Vol. 78 No. 5 ACTA GEOLOGICA SINICA Oct. 2004 1025–1033
http://www.geojournals.cn/dzxbcn/ch/index.aspx

A Tiny Piece of Basalt Probably from Asteroid 4 Vesta

LIN Yangting[1, 2], WANG Daode[2] and WANG Guiqing[2]
1 *Institute of Geology and Geophysics, Chinese Academy of Sciences, Beijing 100090; E-mail: Linyt@mail.igcas.ac.cn*
2 *Guangzhou Institute of Geochemistry, Chinese Academy of Sciences, Guangzhou, Guangdong 510640*

Abstract Grove Mountains (GRV) 99018 is a new eucrite (0.23 g), consisting mainly of pyroxene (50.5 vol%) and plagioclase (37.2 vol%) with minor silica minerals (7.0 vol%) and opaque minerals (5.2 vol%). It was intensely shocked, leading to partial melting, formation of abundant tiny inclusions in pyroxenes and plagioclase, and heavy brecciation. Exsolution of most pyroxenes (1–3 μm in width of the lamellae), recrystallization of the shock-induced melt pockets and veins (5–20 μm in size), and homogeneous compositions of pyroxenes of various occurrences suggest the intense thermal metamorphism of GRV 99018 in the asteroidal body Vesta. This new eucrite will bring additional constraints on the chemical composition and multi-stage thermal and shock history of Vesta.

Key words: meteorite, basalt, eucrite, asteroid, magmatism, shock metamorphism, thermal history

1 Introduction

Eucrites consist mainly of pyroxenes and calcic plagioclase, a kind of extra-terrestrial basalts besides those from the Mars and Moon. They show close affiliation with diogenites (orthopyroxenites) and howardites (mixtures of diogenitic orthopyroxene and eucritic clasts), and these three groups of differentiated meteorites (achondrites) are referred to as the **H**owardite-**E**ucrite-**D**iogenite (HED) clan. The parent body of HED meteorites is probably asteroid 4 Vesta, according to their similar optical reflectance spectral features (Larson and Fink, 1975). Recent discovery of 20 small main-belt asteroids that have distinctive visual and near-infrared spectra similar to those of Vesta and HED meteorites supports the genetic connection between Vesta and HED (Binzel and Xu, 1993). Based on the petrography and mineralogy of HED achondrites, a layered crust model of the parent body of HED was proposed, consisting of an upper crust with extrusive lava-like eucrites that have been brecciated and thermally metamorphosed, cumulate eucrites with varying thickness, and diogenite mantle (Takeda, 1997). Observations of diogenitic orthopyroxene at the bottom of the south polar crater (Thomas et al., 1997) are consistent with a deep diogenitic layer expected by this model. In addition, a wide range of closure temperatures of diogenites suggests repeated excavation of these meteorites from their original sites over a long time interval during cooling (Liermann and Ganguly, 2001).

Studies of eucrites revealed pronounced variation in petrography and mineralogy. These meteorites are classified as the cumulate, noncumulate, and polymict types. Noncumulate eucrites are further divided into the ordinary (monomict or unbrecciated) and surface (lava-like) subtypes (Takeda, 1997). On the other hand, eucrites experienced complicated thermal metamorphism on the crust of Vesta, and they are classified from petrographic type 1 to type 6 with increasing thermal metamorphism (Takeda and Graham, 1991). Although brecciated eucrites are common, only a few samples are probably shock-induced melt rocks or contain melt pockets and veins (e.g. Yamaguchi et al., 1993; Yamaguchi et al., 1997). The presence of shock-induced melts indicates at least a partial contribution of heat by impact during the early history of the HED parent body.

GRV 99018 was collected on blue ice in the Grove Mountains region, Antarctica, by the 16th Chinese Antarctica Research Expedition (CHINARE) in 2000. It is a tiny fragment half covered with dark fusion crust (Fig. 1), and its broken surface is fresh and light gray in color. The piece weighs only 0.23 g. A detailed petrographic and mineral chemical study is conducted in order to clarify the petrogenesis of GRV 99018 and to provide constraints on the evolutional history of the crust of Vesta.

2 Sample and Experiments

The meteorite was chipped into two pieces, and the larger one (0.12 g) was embedded in epoxy and cut into 5 slices using a low-speed diamond saw. One of the slices (GRV 99018-2) was prepared as a polished thin section, and it was studied in this work.

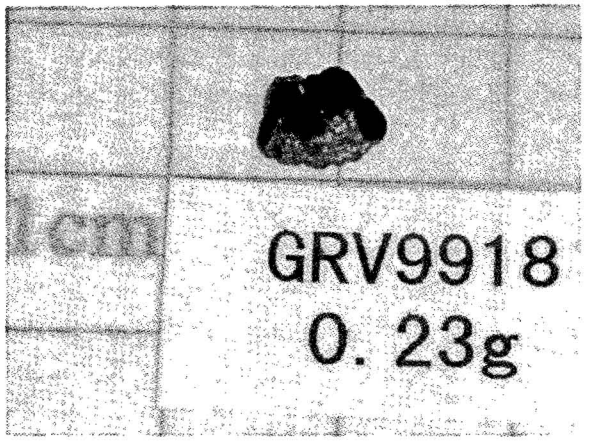

Fig. 1. Photo of GRV 99018, showing a part of dark fusion crust.
Scale of the grid is 1 cm.

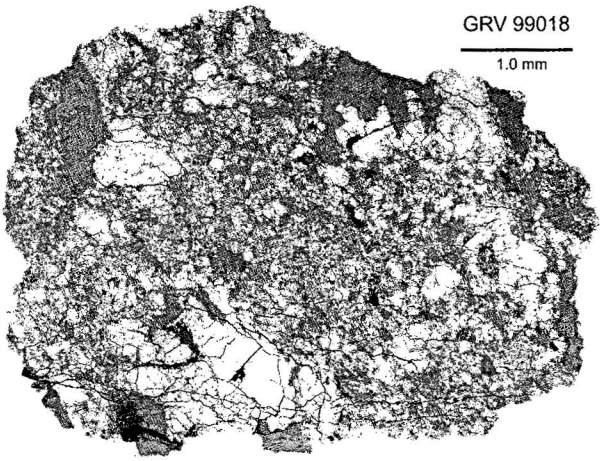

Fig. 2. Back-scattered electron (BSE) image mosaic of GRV 99018, showing a noncumulate monomict brecciated texture.
The dark gray grains are plagioclase and silica minerals (invisible here), and the bright grains are pyroxenes and opaque minerals (indistinguishable, except for a big white troilite grain close to the lower middle edge of the section). Note heavily fractured silicate grains. Width of the view is 5.3 mm.

Beside optical microscope, textural observation was also carried out using a scanning electron microscope (SEM) type JEOL-JSM845 at the Department of Geological Sciences at the Arizona State University, Tempe, USA, and under back-scattered electron image (BSE) model of an electron probe microanalyzer (EPMA) type JEOL 8800 at the Sun Yat-Sen University, Guangzhou. Modal composition of the sample was deduced from the surface areas of individual minerals on the BSE images. Quantitative analyses of the minerals were conducted under the conditions of 15 keV accelerating voltage and 20 nA beam current (except 10 nA for plagioclase), using the same EPMA and another type CAMECA SX 51 at the Institute of Geology and Geophysics, Chinese Academy of Sciences, Beijing. The standards used are silicates and oxides, and the analyses are treated using the Bence-Albee method.

3 Results

3. 1 Petrography

GRV 99018 is a noncumulate monomict brecciated eucrite (Fig. 2). It consists of 50.5 vol% pyroxenes, 37.2 vol % plagioclase, 7.0 vol% silica minerals and 5.2 vol% troilite and ilmenite with accessory phosphate. A few grains of zircon (~5 μm) were found, too. Almost all grains of pyroxenes show exsolution lamellae, with augite lamellae in converted pigeonite and vise versa (Fig. 2a). The exsolved lamellae are usually 1–3 μm, with a few up to 8 μm in size (Fig. 3b). In contrast, a few grains of pigeonite show no exsolution (Fig. 3c), which have no special textural occurrences. In addition, there is a clast consisting of troilite and rounded silicates, and both the pigeonite and augite show no sign of exsolution (Fig. 3d), different from those in the host meteorite.

In the section, there are recrystallized veins and pockets consisting of fine-grained (<10 μm) augite, pigeonite and plagioclase with minor ilmenite and troilite (Fig. 4). 120° junction of the grains can be noticed (Fig. 4a). A few grains of zircon were found in the pockets (Fig. 4b). In addition, either augite or pigeonite rarely shows signs of exsolution, obviously distinguished from the mineral equivalents in the host meteorite. Modal compositions of the pockets vary significantly, from plagioclase predominant to pigeonite-rich and to silica mineral-rich.

Most grains of silicates are highly fractured, except for those in the recrystallized pockets and veins (Fig. 4). The different occurrences of fracturing suggest that the corresponding shock event should be prior to crystallization of these pockets and veins. Another remarkable feature is the presence of abundant tiny inclusions in most grains of plagioclase, augite and pigeonite. Most of the inclusions in plagioclase are probably pyroxenes, whereas those in both pigeonite and augite are probably ilmenite and chromite (Fig. 3a, b). Also different from the host meteorite, the recrystallized pockets and veins are lack of opaque mineral inclusions. Instead, ilmenite and troilite occur as subhedral grains in contact with silicates with 120° junction (Fig. 4a). Undulose extinction is very common in pyroxenes, plagioclase and silica minerals.

3. 2 Mineral chemistry

3.2.1 Pigeonite

As described above, pigeonite shows various occurrences. However, no significant variation in chemical composition has been found among them (Fig. 5). The converted pigeonite has a narrow compositional range of

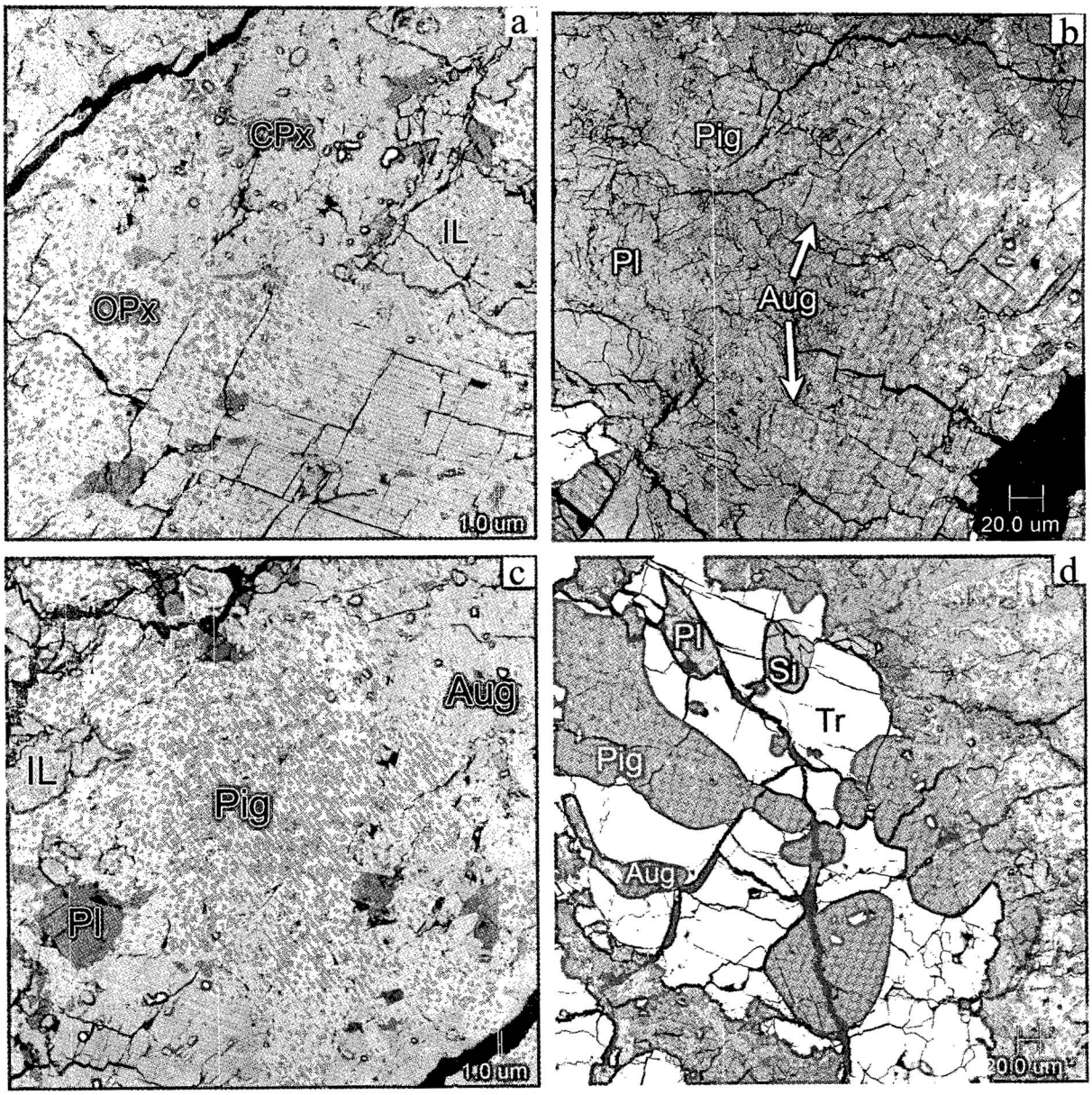

Fig. 3. (a) BSE image showsing exsolution of augite lamellae (dark gray) in converted pigeonite (OPx), and pigeonite lamellae (light gray) in augite (CPx).

Light gray mineral at the right upper corner is ilmenite (IL). Small dark interstitial grains and those in pyroxenes are plagioclase. Abundant tiny light gray inclusions in pyroxenes are probably ilmenite and chromite. Width of the view is 250 μm.

(b) Thick exsolution lamellae of augite in converted pigeonite.

Also note tiny light gray inclusions in pyroxenes and those (probably pyroxenes) in plagioclase. White grain at the lower left is ilmenite. Width of the view is 320 μm.

(c) A clast of pigeonite with almost no exsolution.

Note abundant pigeonite lamellae in the surrounding augite. Width of the view is 170 μm;

(d) A clast consisting of troilite and rounded silicates, including pigeonite, augite, plagioclase and silica.

Note the absence of exsolution of pyroxenes. Width of the view is 480 μm.

$En_{33-39}Fs_{58-65}Wo_{2-9}$, overlapping with small crystals in the recrystallized melt pockets and veins ($En_{34-35}Fs_{62-63}Wo_{2-3}$). In addition, analyses conducted on the cores and rims of large grains of the converted pigeonite, regardless of abundant or few lamellae of augite, indicate relatively homogeneous compositions. An EPMA profile conducted on a pigeonite across a thick lamella of augite shows no significant decrease of CaO toward the interface (Fig. 6). Other minor components are MnO (0.9–1.3 wt%), TiO_2 (<0.30 wt%), Al_2O_3 (<0.24 wt%) and Cr_2O_3 (<0.28 wt%).

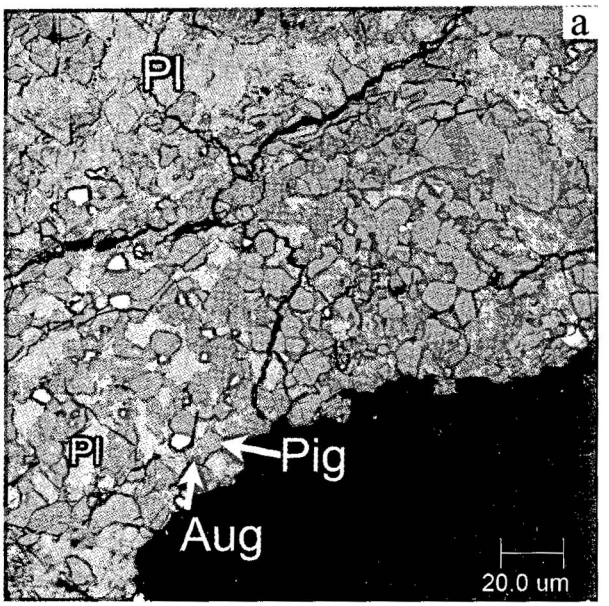

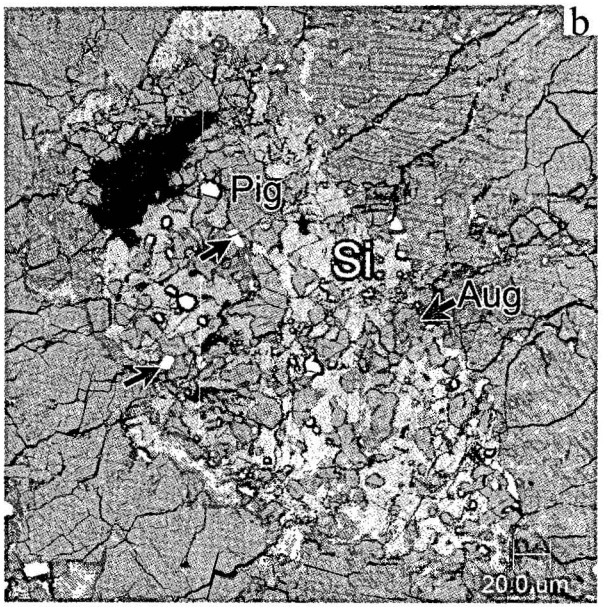

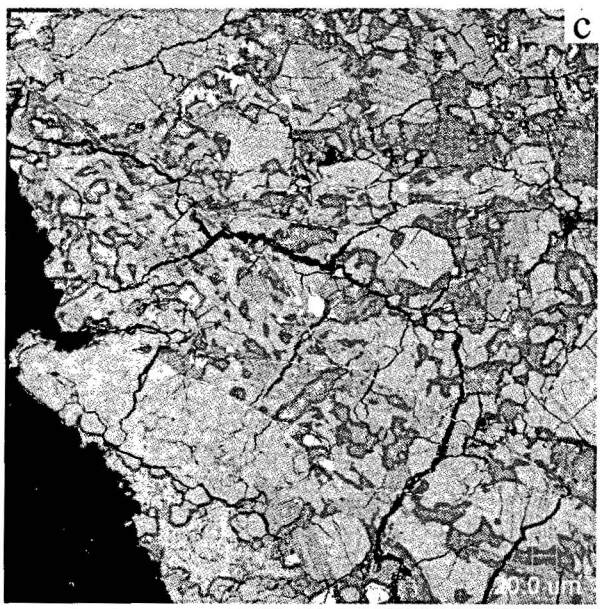

Fig. 4. (a) BSE image of a recrystallized pocket, consisting of pigeonite, augite and plagioclase with minor ilmenite (white spots).
Note 120° junction of the grains and absence of exsolution in both augite and pigeonite. Width of the view is 190 μm.
(b) Another recrystallized pocket with no exsolution of pyroxenes, evidently different from the surroundings.
Two of white grains pointed with arrows are zircon, and others are ilmenite and troilite. Width of the view is 300 μm.
(c) Recrystallized veins (dashed lines) consisting of fine-grained pigeonite, augite and plagioclase.
Width of the view is 480 μm.

The average FeO/MnO ratio (31.8±2.7) is typical of eucrites (30.4), distinctly lower than those of other basalts from the Earth and Moon, although some of the individual analyses overlapping with the range of Mars (Fig. 7). Representative analyses of pigeonite are given in Table 1.

3.2.2 Augite

Augite is also homogeneous in compositions ($En_{28-31}Fs_{25-29}Wo_{41-45}$), without significant differences between individual grains, the lamellae in the converted pigeonite, and the crystals in the recrystallized melt pockets and veins (Fig. 5). The EPMA profile (Fig. 6) across a thick augite lamella (10 μm) shows a very flat pattern. Minor elements are MnO (0.44–0.62 wt%), TiO_2 (0.12–0.29 wt%), Al_2O_3 (0.32–0.49 wt%) and Cr_2O_3 (0.13–0.39 wt%). The FeO/MnO ratios (average 31.0±3.4) are also plotted in the range of eucrites (Fig. 7).

The compositions of both pigeonite and augite before conversion were analyzed using a defocused beam (20 μm in diameter). The results are plotted in Fig. 5, indicating high wollastonite component in pigeonite and high enstatite and ferrosilite components in augite. Higher abundances of minor TiO_2 (0.25–0.72 wt%), Al_2O_3 (0.20–0.75 wt%) and Cr_2O_3 (0.42–0.73 wt%) are probably due to the beam overlapping the tiny inclusions in pyroxenes (e.g. Fig. 3a), because both pigeonite and augite lamellae are poor in these components except for Al_2O_3 in augite.

3.2.3 Plagioclase

Large grains of plagioclase are chemically zoned, with anorthite (An) contents decreasing from the core ($An_{83.7}$) to the rim ($An_{77.4}$). The small grains in the recrystallized melt pockets and veins appear more calcic (An_{85-89}). All analyses are K_2O-poor (<0.26 wt%). Another minor element is FeO, which seems higher in the grains in the pockets (0.51–0.66 wt%) than in the host meteorite (0.05–0.42 wt%). Representative analyses of plagioclase are listed in Table 2.

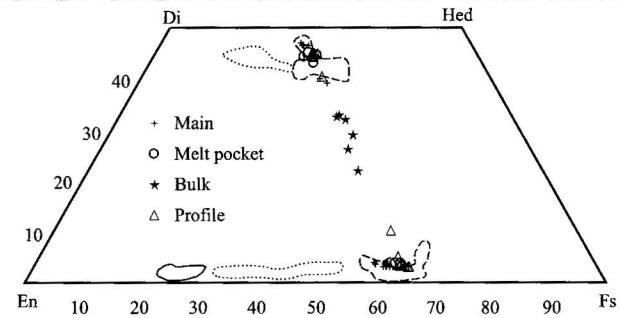

Fig. 5. Triangle diagram of pyroxenes in GRV 99018.
Pigeonite and augite in the recrystallized *Melt pockets* have identical compositions of the counterparts of the *Main* occurrence. Also plotted are *Bulk* grains of pigeonite and augite analyzed by defocused beam and the *Profile* of Fig. 6. Ranges of diogenites (line), cumulate eucrites (dotted line) and ordinary eucrites (dashed line) after (Takeda, 1997).

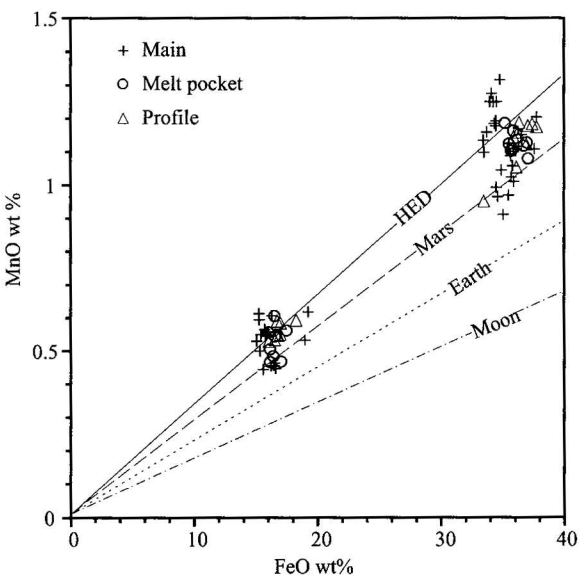

Fig. 7. FeO versus MnO plot of pyroxenes in GRV 99018.
Both pigeonite and augite plot close to the reference line of howardite-eucrite-diogenite (HED). Average FeO/MnO ratios of basaltic pyroxenes from the Earth, Moon, and Mars are shown for comparison.

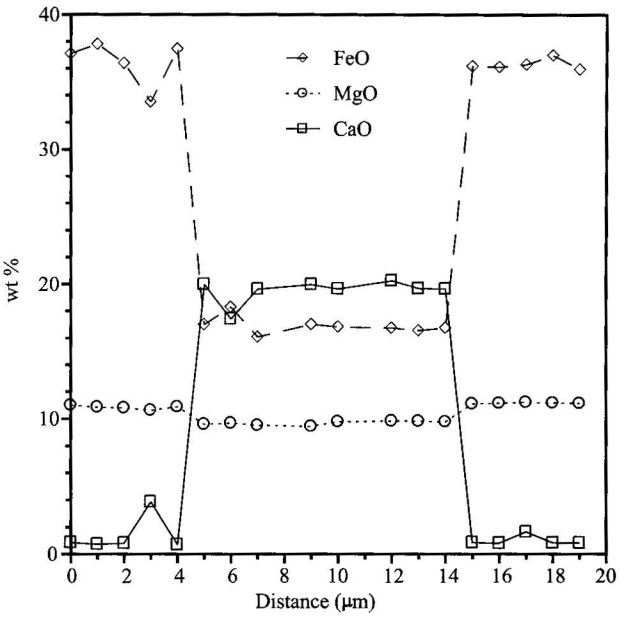

Fig. 6. An EPMA profile of pyroxenes in GRV 99018.
The host pigeonite shows no CaO decreasing toward the interface, and the augite lamella is rather homogeneous in composition.

3.2.4 Others

Ilmenite has homogeneous composition within large grains, and shows no significant variation from grains to grains. Beside major FeO and TiO_2, other minor elements are MnO (0.87–0.98 wt%), CaO (0.13–0.52 wt%), MgO (0.34–0.55 wt%), Cr_2O_3 (0.04–0.22 wt%) and SiO_2 (0.10–0.13 wt%) without detectable Al_2O_3. Table 2 lists the representative analyses of ilmenite. Silica mineral (98.4 wt% SiO_2) contains minor FeO (0.43–0.64 wt%).

4 Discussion

4.1 Classification

The igneous texture and absence of metallic Fe-Ni and chondrules indicate that GRV 99018 is highly differentiated, a typical achondrite. It consists mainly of pyroxenes and plagioclase with minor SiO_2 minerals and ilmenite, within the range of basalts. Calcic plagioclase excludes a Martian origin of GRV 99018, and it is clearly different from GRV 99027 that contains plagioclase with An content of 40–60 mol% and was classified as an lherzolitic shergottite ejected from the Mars (Lin et al., 2002; Lin et al., 2003). Plagioclase in basaltic shergottites is Na_2O-rich, too, and most of the grains have been converted to maskelynite (diaplectic glass) (Lin and Wang, 1995) or shock-induced dense melts (El Goresy et al., 1997). Furthermore, the MnO/FeO ratios of pyroxenes in GRV 99018 are higher than those of Martian basalts (Fig. 7), confirming a different source from the Mars. Although the composition of plagioclase cannot distinguish GRV 99018 from lunar basalts (An_{85-100}), the latter has much low MnO/FeO ratios of pyroxenes in comparison with GRV 99018 (Fig. 7).

On the other hand, the modal composition, the anorthite contents of plagioclase, and the MnO/FeO ratios of pyroxenes in GRV 99018 all are similar with those of eucrites. It is noncumulate, based on the absence of cumulate textures. The ferrosilite contents (Fs) of pyroxenes are within the range of noncumulate eucrite, and are distinctly higher than those of cumulate eucrites (Fig. 5). GRV 99018 is brecciated, but monomict instead of polymict, because no other lithic clasts have been found in the section. The recrystallized textures and identical mineral chemistry of the pockets and veins in comparison with those of the host meteorite suggest that these pockets and veins crystallized from shock-induced melts instead of polymict clasts. Hence, GRV 99018 is classified as

Table 1 Representative analyses of pigeonite and augite in GRV 99018 (wt%)

	Augite					Pigeonite					
	1°	2°	3§	4§	5*	6°	7°	8§	9	10	11*
SiO_2	51.1	51.1	51.7	51.8	49.0	49.1	49.8	49.9	50.4	49.3	49.2
TiO_2	0.18	0.22	0.23	0.26	0.43	0.11	0.08	0.19	0.16	0.10	0.30
Al_2O_3	0.34	0.36	0.41	0.45	0.38	0.07	0.09	0.09	0.20	0.15	0.26
Cr_2O_3	0.17	0.17	0.17	0.22	0.73	0.04	0.05	0.08	0.07	0.10	0.42
FeO	17.5	16.2	16.2	16.4	22.2	35.8	37.1	36.3	35.9	34.9	27.0
MnO	0.56	0.46	0.45	0.46	0.69	1.10	1.13	1.12	1.01	1.05	0.85
MgO	10.2	9.82	9.83	9.83	10.21	11.2	11.4	11.5	12.2	11.7	10.6
CaO	19.5	19.7	20.4	20.1	14.0	0.78	0.99	0.74	1.06	0.84	9.16
Na_2O	n.d.	0.09	0.09	0.10	0.09	n.d.	n.d.	n.d.	n.d.	n.d.	n.d.
Total	99.59	98.16	99.47	99.58	97.78	98.17	100.57	99.94	101.00	98.12	97.81
	Cations per six oxygens										
Si	1.984	2.001	1.997	1.999	1.964	2.003	1.994	2.002	1.993	2.006	1.984
Ti	0.005	0.007	0.007	0.007	0.013	0.003	0.002	0.006	0.005	0.003	0.009
Al	0.016	0.016	0.019	0.021	0.018	0.003	0.004	0.004	0.009	0.007	0.012
Cr	0.005	0.005	0.005	0.007	0.023	0.001	0.002	0.003	0.002	0.003	0.013
Fe	0.569	0.531	0.525	0.531	0.744	1.221	1.240	1.217	1.188	1.187	0.911
Mn	0.018	0.015	0.015	0.015	0.023	0.038	0.038	0.038	0.034	0.036	0.029
Mg	0.589	0.574	0.567	0.566	0.610	0.685	0.677	0.686	0.720	0.706	0.638
Ca	0.811	0.828	0.845	0.830	0.603	0.034	0.042	0.032	0.045	0.036	0.396
Na	0.002	0.007	0.006	0.007	0.007	0.003	0.001	0.000	0.000	0.001	0.002
En mol%	29.9	29.7	29.3	29.4	31.2	35.3	34.6	35.5	36.9	36.6	32.8
Wo mol%	41.2	42.9	43.6	43.1	30.8	1.8	2.2	1.6	2.3	1.9	20.3
Fs mol%	28.9	27.5	27.1	27.6	38.0	63.0	63.3	62.9	60.8	61.5	46.9

Note: ° in melt pockets, § exsolution lamellae, * defocused beam analyses, 9 rim, 10 core.

noncumulate monomict brecciated eucrite based on the scheme proposed by Takeda (1997). Furthermore, the $mg^{\#}$ values (Mg × 100/(Mg+Fe), atomic), chemical homogeneity and micro-scale exsolution of pyroxenes of GRV 99018 suggest its affinity to ordinary eucrites (Takeda, 1997), different from lava-like surface eucrites that show TEM scale exsolution and significant compositional zoning features of pyroxenes.

4.2 Petrogenesis of GRV 99018

Based on the petrography and mineral chemistry, a model of formation and evolution of GRV 99018 is summarized in order as: (1) Crystallization of the parent magma of GRV 99018 at site close to the surface of Vesta; (2) A heavy shock event partially melted the meteorite and brecciated it. The meteorite was probably dug out from depth, then buried with a thick layer of regolith; (3) The meteorite experienced a high degree of thermal metamorphism after burial in the regolith; (4) Another impact event, which is related to the common undulose extinction of silicates, ejected the sample into an Earth-crossed orbit. Evidence for the above scenario is discussed below.

The noncumulate texture and small grain sizes of GRV 99018 (except for a few clasts with grain sizes up to 0.5 mm) suggest that it crystallized at depth between the cumulate and surface (or lava-like) types of eucrites. However, detailed information on the igneous processes of GRV 99018 has strongly been erased by the later shock events and the subsequent strong thermal metamorphism. Similar compositions of pyroxenes of various occurrences indicate that they have achieved equilibration through Ca diffusion between pigeonite and augite at low temperatures, representative of no longer the original compositions determined by crystallization. In order to access the original compositions of pyroxenes, a defocused beam (20 μm in diameter) was used to analyze the bulk compositions of the converted pigeonite and augite. The analyses (Fig. 5, Table 1) gave crystallization temperatures of 1100±40°C, based on the two-pyroxene thermometer (Lindsley and Andersen, 1983). After crystallization, the rock experienced slow cooling in order to form the micrometer-

Table 2 Representative analyses of plagioclase, ilmenite and silica mineral in GRV 99018 (wt%)

	Plagioclase						Ilmenite			Silica
	1'	2'	3#	4#	5°	6°	7	8°	9°	10
SiO_2	48.9	48.1	47.3	47.1	46.0	45.5	0.12	0.13	0.11	98.06
TiO_2	0.04	0.02	0.03	0.03		0.07	51.6	50.6	50.6	
Al_2O_3	32.2	32.8	33.8	33.5	34.3	34.0		0.05	0.01	0.01
Cr_2O_3	0.03		0.01	0.01	0.01	0.02	0.04	0.15	0.20	
FeO	0.25	0.15	0.08	0.05	0.51	0.66	45.1	45.9	45.6	0.43
MnO			0.01	0.03			0.98	0.93	0.94	
MgO	0.02	0.01	0.01	0.01	0.02	0.07	0.55	0.34	0.36	0.01
CaO	15.3	15.6	16.8	16.7	17.4	17.6	0.13	0.50	0.50	0.07
Na_2O	2.31	2.29	1.79	1.80	1.26	1.12	0.02	0.02	0.04	0.03
K_2O	0.26	0.12	0.03	0.11	0.03	0.09		0.03	0.02	
Total	99.30	99.19	99.84	99.29	99.63	99.24	98.67	98.72	98.50	98.64
					Cations per formula					
Si	2.252	2.220	2.171	2.175	2.128	2.118	0.003	0.003	0.003	0.997
Ti	0.001	0.001	0.001	0.001	0.000	0.002	0.988	0.968	0.970	0.000
Al	1.747	1.785	1.832	1.825	1.869	1.866	0.000	0.002	0.000	0.000
Cr	0.001	0.000	0.000	0.000	0.000	0.001	0.001	0.003	0.004	0.000
Fe	0.010	0.006	0.003	0.002	0.020	0.025	0.960	0.976	0.972	0.004
Mn	0.000	0.000	0.000	0.001	0.000	0.000	0.021	0.020	0.020	0.000
Mg	0.002	0.001	0.000	0.000	0.001	0.005	0.021	0.013	0.014	0.000
Ca	0.758	0.773	0.825	0.825	0.861	0.879	0.003	0.013	0.014	0.001
Na	0.206	0.205	0.159	0.161	0.113	0.101	0.001	0.001	0.002	0.001
K	0.015	0.007	0.002	0.006	0.002	0.005	0.000	0.001	0.000	0.000
Sum	4.992	4.997	4.993	4.998	4.996	5.002	2.000	2.000	2.000	1.003
An mol%	77.4	78.5	83.7	83.1	88.3	89.2				

Note: ' rim, # core, ° in melt pockets.

scale exsolution of pyroxenes. Closure temperature of pyroxenes (below that temperature diffusion between pyroxenes ceased substantially) can be determined from the compositions of augite lamellae and converted pigeonite (Fig. 5, Table 1) using the two-pyroxene thermometer, and it is 500–600°C. In addition, the maximum width of augite lamellae in the converted pigeonite in GRV 99018 is compatible with that reported in the Ibitira noncumulate eucrite (~ 7 μm in width, Miyamoto et al., 2001), one of the most heavily thermal metamorphosed eucrites. Hence, we suggest a similar cooling rate for GRV 99018 as that of Ibitira, which was estimated to cool at a rate of 0.02 °C/year between 1082–550 °C based on the width and the zoning profile of augite lamellae (Miyamoto et al., 2001). The cooling took place before the brecciation according to the textural relationship between the exsolved lamellae and cracks. The exsolved lamellae of pyroxenes were cut by cracks, whereas there is no evidence for termination of exsolved lamellae by the cracks (e.g. Fig. 3), indicating the exsolution prior to the brecciation.

Beside brecciation, the heavy shock event caused partial melting of the rock, as indicated by the presence of the recrystallized melt pockets and veins. The large sulfide assemblage with rounded silicate inclusions (Fig. 3d) also suggests crystallization from melts that could be produced by the impact, too. Another result of partial melting is related to the abundant tiny inclusions in most pigeonite, augite and plagioclase. The flat zoning profile of augite lamellae in the converted pigeonite (Fig. 6) indicates no significant heating effect after the exsolution, different from the report about a reheating and subsequent rapid cooling of Ibitira based on Ca gradient near the interface between augite and pigeonite (Miyamoto et al., 2001). One possibility is that the impact heating is highly heterogeneous and the zoning profile of augite lamellae was not affected. Another scenario is that subsequent slow cooling has erased the sudden reheating effect. This is supported by recrystallization of the melt pockets and veins. The recrystallization should take place after the shock event, since these pockets and veins are lack of

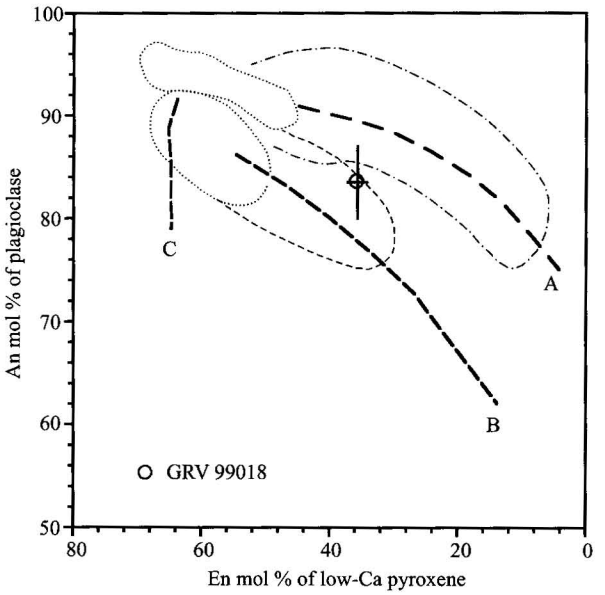

Fig. 8. Average anorthite (An) content of plagioclase plots versus average enstatite (En) content of low-Ca pyroxene in GRV 99018.

Note GRV 99018 locates between the Na_2O-poor (A) and Na_2O-rich (B) crystallization trends of HED meteorites. Error bars are 1σ. Literature is after Takeda (1997).

brecciation. Another evidence for a high degree of thermal metamorphism after the main impact is the nearly identical compositions of pigeonite and augite in the pockets and veins in comparison with those as exsolved lamellae (Fig. 5). The intense thermal metamorphism can be explained by burial in a thick layer of hot ejecta. In the case of a fast cooling after the main impact, much higher closure temperatures would have been expected for the pyroxenes in the pockets and veins.

Finally, GRV 99018 was ejected from Vesta into space by another impact event. Undulose exsolution of silicates is related with this event.

4.3 Comparison with other noncumulate eucrites

As discussed above, GRV 99018 is classified as noncumulate monomict brecciated eucrite. Its modal composition, mineral chemistry, closure temperatures of pyroxenes and estimated cooling rate are within the ranges of those for noncumulate eucrites. However, GRV 99018 experienced strong shock metamorphism. The rock was partially melted by the shock event. Although brecciation of eucrites is common, impact melt veins were reported only in a few eucrites (e.g. Yamaguchi et al., 1993). In addition, Y-790447 is probably a shock-induced melt rock (Yanai and Kojima, 1995). Discovery of the new heavily shocked eucrite and the correlated intense thermal metamorphism suggests that impact was probably an important heating source during the early evolutional history of Vesta. This is supported by recent reports of extensive impact melting asteroidal bodies of ordinary chondrites during the cataclysmic bombardment of the early solar system (Folco et al., 2004). Short-lived radionuclides are used to being referred to as one of the main heating sources of planets and asteroids (Zinner, 2003). However, recent study of ^{26}Al in chondrules from a primitive CO3.0 chondrite reveals relatively low initial $(^{26}Al/^{27}Al)_0$ ratios, requiring for additional heating sources of melting asteroids (Kunihiro et al., 2004).

Another difference of GRV 99018 from other noncumulate eucrites is demonstrated in Fig. 8. Three hypothetical crystallization trends of the HED meteorites have been recognized (Takeda, 1997), whereas GRV 99018 is plotted at the middle of the Na_2O-poor (A) and Na_2O-rich (B) trends. It may indicate a different magma source, but more studies are required to characterize the parent magma of GRV 99018.

5 Conclusions

GRV 99018 consists mainly of pyroxenes and plagioclase with minor silica minerals, troilite, ilmenite and phosphate. It is highly brecciated but monomict. According to the mineral chemistry and exsolution textures of pyroxenes, GRV 99018 probably started to crystallize from liquid at ~1100±50 °C, followed by a slow cooling process after solidification. This meteorite is classified as a noncumulate brecciated eucrite and belongs to the "ordinary" type, although it shows different correlations between An contents of plagioclase and En contents of pyroxene. GRV 99018 is the first small piece of basalt that was probably ejected from asteroid 4 Vesta and found in the Grove Mountains, Antarctica.

Discovery of the recrystallized melt pockets and veins and presence of the abundant tiny inclusions in most pyroxenes and plagioclase revealed a high degree of shock metamorphism. The evidence for shock melting and subsequent strong thermal metamorphism suggests that impact heating may play an important role in differentiation of asteroids, such as Vesta.

After the main impact, GRV 99018 was probably buried in a thick layer of hot ejecta, and experienced strong thermal metamorphism with a slow cooling rate. This thermal metamorphism caused the melt pockets and veins to recrystallize, and homogenized the chemical compositions of pyroxenes of various occurrences. The closure temperatures of pyroxenes are ~500–600 °C according to the two-pyroxene thermometer. Our results confirm an intense thermal metamorphism during the crust evolution of Vesta.

Acknowledgements

We are grateful to Drs. Guan Yunbin and Xu Ping for their assistance in laboratories. This study is supported by the National Natural Science Foundation of China (Grant No. 40232026) and the pilot project of knowledge-innovation program of the Chinese Academy of Sciences (Grant No. KZCX3-SW-123).

Manuscript received June 17, 2004
accepted Sept. 12, 2004
edited by Xie Guanglian

References

Binzel, R.P., and Xu, S., 1993. Chips off of asteroid 4 Vesta: Evidence for the parent body of basaltic achondrites. *Science,* 260: 186–191.

El Goresy, A., Wopenka, B., Chen, M., and Kurat, G., 1997. The saga of maskelynite in Shergotty (abstract). *Meteorit. Planet. Sci.,* 32: A38–39.

Folco, L., Bland, P.A., D'Orazio, M., Franchi, I.A., Kelley, S.P., and Rocchi, S., 2004. Extensive impact melting on the H-chondrite parent asteroid during the cataclysmic bombardment of the early solar system: Evidence from the achondritic meteorite Dar al Gani 8961. *Geochim. Cosmochim. Acta,* 68: 2379–2397.

Kunihiro, T., Rubin, A.E., McKeegan, K.D., and Wasson, J.T., 2004. Initial $^{26}Al/^{27}Al$ in carbonaceous-chondrite chondrules: too little ^{26}Al to melt asteroids. *Geochim. Cosmochim. Acta,* 68: 2947–2957.

Larson, H.P., and Fink, U., 1975. Infrared spectral observations of Asteroid 4 Vesta. *Icarus,* 26: 420–427.

Liermann, H.-P., and Ganguly, J., 2001. Compositional properties of coexisting orthopyroxene and spinel in some Antarctic diogenites: Implications for thermal history. *Meteorit. Planet. Sci.,* 36: 155–166.

Lin Yangting and Wang Daode, 1995. Inspiration from study of Antarctic meteorites VI: Martian meteorites and their cosmochemical significances. *Antarct. Res.,* 7: 35–52 (in Chinese).

LinYangting, Wang Daode, Miao Bingkui, Ouyang Ziyuang, Liu Xiaohan and Ju Yitai, 2003. Grove Mountains (GRV) 99027: A new Martian meteorite. *Chinese Sci. Bull.,* 48: 1771–1774.

Lin, Y., Ouyang, Z., Wang, D., Miao, B., Liu, X., Kimura, M., and Jun, Y., 2002. Grove Mountains (GRV) 99027: A new martian lherzolite. *Meteorit. Planet. Sci.,* 37: A87.

Lindsley, D.H., and Andersen, D.J., 1983. A two-pyroxene thermometer. *Proc. Lunar Planet. Sci. Conf.* 14th: A887–A906.

Miyamoto, M., Mikouchi, T., and Kaneda, K., 2001. Thermal history of the Ibitira noncumulate eucrite as Inferred from pyroxene exsolution lamella: evidence for reheating and rapid cooling. *Meteorit. Planet. Sci.,* 36: 231–237.

Takeda, H., 1997. Mineralogical records of early planetary processes on the HED parent body with reference to Vesta. *Meteorit. Planet. Sci.,* 32: 841–853.

Takeda, H., and Graham, A. L., 1991. Degree of equilibration of eucritic pyroxenes and thermal metamorphism of the earliest planetary crust. *Meteoritics,* 26: 129–134.

Thomas, P.C., Binzel, R.P., Gaffey, M.J., Storrs, A.D., Wells, E. N., and Zellner, B.H., 1997. Impact excavation on asteroid 4 Vesta: Hubble Space Telescope results. *Science,* 277: 1492–1495.

Yamaguchi, A., Mori, H., and Takeda, H., 1993. Mineralogy and Shock Textures in the Padvarninkai Eucrite. *Meteoritics,* 28: 462.

Yamaguchi, A., Taylor, G.J., and Keil, K., 1997. Shock and thermal history of equilibrated eucrites from Antarctica. *Antarct. Meteorite Res.,* 10: 415.

Yanai, K., and Kojima, H., 1995. Catalog of the Antarctic Meteorites, 230pp. National Institute of Polar Research.

Zinner, E., 2003. An isotopic view of the early solar system. *Science,* 300: 265–267.